
Graph Neural Networks for Motion Planning

Arbaaz Khan^{1,2*}, Alejandro Ribeiro¹, Vijay Kumar¹ and Anthony G. Francis²

Abstract

This paper investigates the feasibility of using Graph Neural Networks (GNNs) for classical motion planning problems. Planning algorithms that search through discrete spaces as well as continuous ones are studied. This paper proposes using GNNs to guide the search algorithm by exploiting the ability of GNNs to extract low level information about the topology of a planning space. We present two techniques, GNNs over dense fixed graphs for low-dimensional problems and sampling-based GNNs for high-dimensional problems. We examine the ability of a GNN to tackle planning problems that are heavily dependent on the topology of the space such as identifying critical nodes, learning a heuristic that guides exploration in A^* , and learning the sampling distribution in Rapidly-exploring Random Trees (RRT). We demonstrate that GNNs can offer better results when compared to traditional analytic methods as well as learning-based approaches that employ fully-connected networks or convolutional neural networks.

1 Introduction

Motion planning is a widely studied problem with applications in many fields such as robotics, computer graphics and medicine [1]. Early planning methods such as Dijkstra’s operate by searching a discretized version of the space of interest. The number of states required to cover a space can explode exponentially as the dimensionality of the space increases. A^* looks to improve upon Dijkstra’s by employing a heuristic that can inform the search [2]. However, designing a heuristic is in itself a challenging problem [3]. Further, in scenarios such as robotics, discretization can possibly lead to situations that violate kinodynamic constraints of the robot. Sampling-based Planners (SBPs) such as Rapidly-exploring Random Trees (RRTs) look to overcome this drawback by directly approximating the topology of the configuration space (C-space), i.e the space of all possible agent configurations. These methods construct a graph or tree by sampling points in C-space and connecting these points in the graph if a collision free trajectory is feasible [4]. A caveat of SBPs is that the number of samples required to uniformly cover a space increases with the dimensionality of the C-space [5].

Recently, researchers have attempted to address the shortcomings of these methods by using deep learning to identify samples in C-space which are in some sense more important. For example, for a robot navigating an office space, samples in narrow corridors are more important than samples in free space. Ichter et.al [6] propose using the latent space of a conditional variational autoencoder (CVAE) to bias the sampling process towards these critical samples in a SBP. RL-RRT [7] proposes using deep reinforcement learning (RL) to bias tree-growth towards promising regions of the C-space, [8] use RL to learn an implicit sampling distribution to reduce the overall number of samples required. Critical PRMs [9] look to directly learn these critical samples while LEGO [10] focuses on learning critical samples for graph search algorithms such as A^* .

A common theme among these is the use of convolutional neural networks (CNNs) or fully-connected networks (FCNs) to learn information about the planning space. Instead in this paper we argue

*1 Authors are with GRASP Lab, University of Pennsylvania, USA and 2 authors are with Google Brain. {arbaazk@seas.upenn.edu}

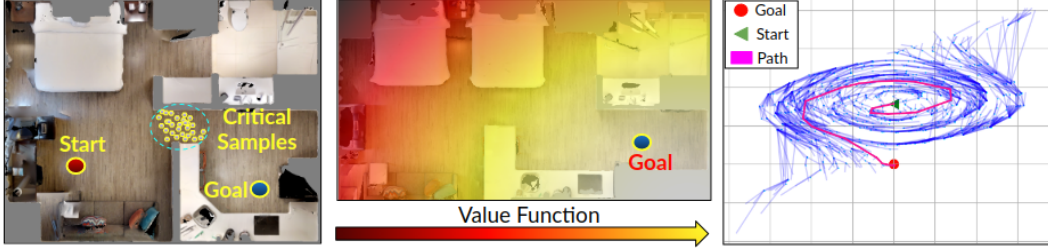


Figure 1: **Graph Neural Networks for Motion Planning.** a) Identifying critical samples for a specified start and goal. b) Value function approximation for a given planning space. c) GNN based sampler to guide tree-growth in RRT for a pendulum.

that most planning spaces have rich topological structure which need not necessarily lie on a two dimensional lattice. When using a CNN or FCN, much of the information about this structure is lost, and the results we show demonstrate that significant changes to the underlying structure of the environment can result in poor generalization of methods that use CNNs and FCNs. Graph Neural Networks (GNNs) have attracted immense attention in the machine learning community. They have been applied successfully to problems that have rich underlying graphical structure such as text classification [11], protein interface prediction [12], parsing social relationships [13], large scale multi-agent reinforcement learning [14]. This work hypothesizes that GNNs can potentially offer better solutions than existing learning methods or naive heuristics for planning problems where the topology of the C-space is an irregular graph. It has also been shown in the past that GNNs are invariant to graph permutations or isomorphisms [15]. We further hypothesize that this property can be exploited to transfer GNN-based planners to new unseen environments. Concretely, this paper proposes GNN solutions to the following suite of motion planning problems;

- **Identifying Critical Samples** Given a static dense graph that covers the C-space of interest, a GNN is trained to identify critical nodes relevant to a given planning problem (Fig 1a)). The quality of critical samples computed by the GNN architectures is compared against those produced by CNNs, or by sampling the latent space of a (CVAE) as in [10].
- **Graph Neural Networks as Value Functions** Given a static dense graph that covers the C-space of interest, a GNN is trained to predict the value or cost to go from a given node to a specified goal node which can be used as a heuristic by a planning algorithm (Fig 1b)). On analyzing relevant metrics, the GNN based heuristic is shown to outperform the L2 heuristic as well as CNN based heuristics.
- **Sampling with Graph Neural Networks** A GNN is used to compute the parameters of the sampling distribution from which the samples are drawn to expand the graph in a SBP (Fig 1c)). We investigate the efficacy of the GNN sampler against a uniform sampler and show that the GNN based sampler is able to guide the search tree towards the goal node faster.

We experimentally demonstrate that GNNs outperform existing solutions and in some cases even improve upon analytic methods for machine learning in motion planning.

2 Preliminaries

In this section, we outline some of the notation used across the planning problems considered in this paper along with a brief overview of GNNs. Let $\mathcal{X} \in \mathbb{R}^d$ represent a d -dimensional C-space. \mathcal{X}_{obs} denotes the part of the space occupied by obstacles that can cause collisions. Thus, free space is given as $\mathcal{X}_{\text{free}} = \mathcal{X} \setminus \mathcal{X}_{\text{obs}}$. Let the initial condition be $x_{\text{init}} \in \mathcal{X}_{\text{free}}$ and the goal condition given as $x_g \in \mathcal{X}_{\text{free}}$. The path \mathbf{p} is said to be feasible if it is collision free $\mathbf{p}(\zeta) \in \mathcal{X}_{\text{free}} \forall \zeta \in [0, 1]$ and if $\mathbf{p}(0) = x_{\text{init}}$, $\mathbf{p}(1) = x_{\text{goal}}$. Let there also exist a cost function $c(p)$ that maps the path \mathbf{p} to a bounded cost $[0, c_{\text{max}}]$. A motion planning problem \mathbf{M} is represented as the tuple, $\mathbf{M} = \{\mathcal{X}_{\text{free}}, x_{\text{init}}, x_{\text{goal}}\}$. In subsequent sections, we build on this notion of the planning problem to achieve different objectives.

2.1 Graph Neural Networks

GNNs can be seen as generalizations of CNNs to general graphs by employing convolutional graph filters [16]. Consider a graph $\mathcal{G} = (\mathbf{V}, \mathbf{E})$ described by a set of N nodes denoted as \mathbf{V} , and a set of edges denoted by $\mathbf{E} \subseteq \mathbf{V} \times \mathbf{V}$. Let this graph act as support for data $\mathbf{x} = [\mathbf{x}_1, \dots, \mathbf{x}_N] \in \mathbb{R}^{N \times m}$. The relationship between \mathbf{x} and \mathcal{G} can be completely characterized by a matrix \mathbf{S} called the graph shift operator. The elements of \mathbf{S} given as s_{ij} respect the sparsity of the graph, i.e $s_{ij} = 0, \forall i \neq j$ and $(i, j) \notin \mathbf{E}$. Examples for \mathbf{S} are the adjacency matrix, the graph laplacian, and the random walk matrix. \mathbf{S} can be used to define the map $\mathbf{y} = \mathbf{S}\mathbf{x}$. If the set of neighbors of node n is given by \mathcal{B}_n then the operation $[\mathbf{S}\mathbf{x}]_n = \sum_{j=n, j \in \mathcal{B}_n} s_{nj} \mathbf{x}_n$ performs a simple aggregation of data at node n from its neighbors that are one hop away. Recursively, one can access information from nodes located further away. For example, $\mathbf{S}^k \mathbf{x} = \mathbf{S}(\mathbf{S}^{k-1} \mathbf{x})$ aggregates information at each node from its k -hop neighbors. Using this map, the spectral K -localized graph convolution is defined as:

$$\mathbf{z} = \sum_{k=0}^K h_k \mathbf{S}^k \mathbf{x} = \mathbf{H}(\mathbf{S}) \mathbf{x} \quad (1)$$

where $\mathbf{H}(\mathbf{S}) = \sum_{k=0}^{\infty} h_k \mathbf{S}^k$ is a linear shift invariant graph filter [17] with coefficients h_k . In practice, the output of a graph convolutional filter is followed by a nonlinearity σ to produce \mathbf{y} . Thus, the output at the first layer is given as:

$$\mathbf{y}_1 = \sigma \left[\mathbf{z}_1 \right] = \sigma \left[\sum_{k=0}^K h_{1k} \mathbf{S}^k \mathbf{x} \right]. \quad (2)$$

where h_{1k} are the filter coefficients of the first layer. In general, there are a total of L layers each of which produces output the \mathbf{y}_L according to the recursion

$$\mathbf{y}_L = \sigma \left[\mathbf{z}_L \right] = \sigma \left[\sum_{k=0}^K h_{Lk} \mathbf{S}^k \mathbf{y}_{L-1} \right]. \quad (3)$$

Eqns 2 and 3 outline the main graph convolution operations. There exist several variants of GNNs that build on these basic graph convolutions such as Graph Attention Transformers (GATs) [18] that we employ in this paper.

3 Learning Critical Samples with Graph Neural Networks

Consider a graph $\mathcal{G} = (\mathbf{V}, \mathbf{E}, \mathbf{W})$ covering the d -dimensional configuration space $\mathcal{X} \in \mathbb{R}^d$. The set of vertices \mathbf{V} represents a collection of points in \mathbb{R}^d , \mathbf{E} represent edges between these points and edge weights between node u and v given by $w_{uv} \in \mathbf{W}$ is the cost of traversing the edge. Each node n is equipped with a feature representation $\mathbf{x}_n \in \mathbb{R}^m$. For example, in a two-dimensional planning problem, vertices are randomly sampled points in the space with edge connections based on some k -nearest neighbor rule and node n 's features can consist of its own xy position, x_{init} and x_{goal} . This choice of features is arbitrary and without loss of generalization can be adapted to suit the problem. Collectively, for the full graph, the feature vector is given as $\mathbf{x} = [\mathbf{x}_1, \dots, \mathbf{x}_N]$ where N is the cardinality of the graph. In this section and section 4, we are interested in using a graph that covers the configuration space \mathbb{R}^d in a uniform manner. It has been shown in the past that a non-lattice, low dispersion sampling scheme such as a Halton sequence is ideal for uniform coverage [19], and thus, we choose \mathcal{G} to be a r -disc Halton graph. In order to uniformly cover \mathbb{R}^d , \mathcal{G} must be sufficiently large/dense. It must be noted that \mathcal{G} remains **constant** even if the planning problem is changed, i.e all planning problems in \mathbb{R}^d can be represented on \mathcal{G} .

Given a graph \mathcal{G} and planning problem $\mathbf{M} = \{\mathcal{X}_{\text{free}}, x_{\text{init}}, x_{\text{goal}}\}$, let there exist a graph search algorithm $\mathbf{A}(\mathcal{G}, \mathbf{M})$ that finds a path \mathbf{p} on \mathcal{G} that is feasible and has the lowest cost if one exists. However, it is often expensive to run the graph search algorithm \mathbf{A} on a dense graph such as \mathcal{G} . To overcome this, we hypothesize that the complexity of a given planning problem can be reduced by identifying only those $\hat{\mathbf{y}}$ nodes in \mathcal{G} that are relevant or *critical*. In practice, once these critical nodes are identified, they can be composed with a sparse graph \mathcal{G}_s on which it is easier to execute \mathbf{A} than on the original dense graph \mathcal{G} . Defining which nodes are *critical* is itself a challenging research problem [9]. In this work, we use the Bottleneck Node algorithm proposed in [10] (Alg 1) to generate the

ground truth critical nodes required for training data due to its guarantees to generate highest cost nodes ("critical") along the shortest path. A drawback of the BN ground truth algorithm is that it needs the shortest path as input. These ground truth samples are denoted as \mathbf{y}_g . Thus, the critical sample problem considered in this paper is:

Problem 1. *Given a motion planning problem \mathbf{M} , a constant graph \mathcal{G} which is the support for feature vector \mathbf{x} , compute critical nodes $\hat{\mathbf{y}} := \pi_\theta(\mathcal{G}, \mathbf{x}, \mathbf{M})$ where π is parametrized by θ ;*

$$\theta^* = \underset{\theta}{\operatorname{argmin}} \|\hat{\mathbf{y}} - \mathbf{y}_g\| \quad (4)$$

We make one approximation to Problem 1. Instead of predicting critical nodes in the graph, we directly predict states in the d -dimensional configuration space, $\hat{\mathbf{y}} \in \mathcal{X}$. This reduces the problem to a simpler regression instead of the immensely more complex structured prediction problem over a large graph. A similar strategy for identifying critical nodes is used in [9, 10].

3.1 Graph Neural Network Architectures

We propose three architectures (Fig 2) to study the abilities of GNNs to identify these critical samples. The first one consists of a simple feedforward graph neural network (Fig 2a) and we call this GNN. Here, the input to the GNN is a static graph \mathcal{G} that has enough nodes to cover \mathbb{R}^d and features associated with each of those nodes. The graph convolutional filters aggregate information at each node from their K -nearest neighbors as given in Eqn 2. Each extra graph convolutional layer provides information from neighbors multiple hops away. For example, in a 2 layer GNN, node n aggregates information from its own neighbors as well as indirect information about its neighbors' neighbors. The GNN architecture also consists of a graph maxpool at the end followed by a FCN layer which predicts one critical state $\hat{\mathbf{y}}$.

The second architecture investigated is the Graph Attention Transformer or GAT [18] (Fig 2b). GATs are similar to GNNs in their use of graph convolutional filters, but instead of aggregating information over all neighbors as in Eqn. 2, information from node n 's neighbors is scaled by a learned attention weight. We hypothesize that when tasked with planning on a dense graph, GATs might benefit from the attention mechanism and focus only on nodes that are critical. However, information about which neighbors to attend to comes at the expense of having to compute additional parameters to produce the aforementioned attention weights and thus GATs tend to be slower during training as well as inference. As before, the output of the GAT $\hat{\mathbf{y}}$, represents a single point in the C-space.

The last architecture we investigate is a modified conditional variational auto-encoder [20] we call GNN-CVAE. The GNN-CVAE consists of two components, an encoder and a decoder. The encoder is made up of GNN layers with a maxpool and a FCN layer at the end. The input to the encoder is the ground truth critical nodes \mathbf{y} and the graph \mathcal{G} . The conditioning variable for the encoder is the feature vector \mathbf{x} which represents parameters of the planning problem at each node. Let the latent variable be denoted by $\tau \in \mathbb{R}^P$. Then, the GNN layers of the encoder map (\mathbf{y}, \mathbf{x}) to parameters $\phi = [\mu, \Sigma]$ of a gaussian distribution in latent space given by $q_\phi(\tau|\mathbf{x}, \mathbf{y}, \mathcal{G})$. The target distribution is fixed to the isotropic normal distribution $\mathcal{N}(0, I)$. The decoder has a similar architecture as the encoder and looks to map a sample from $\mathcal{N}(0, I)$ conditioned on a planning problem's parameters \mathbf{x} and graph \mathcal{G} to the probability distribution of the critical nodes $p_\Theta(\hat{\mathbf{y}}|\tau, \mathbf{x}, \mathcal{G})$ parametrized by Θ . The encoder is used only to train the decoder by minimizing the approximate variational lower bound or the Evidence Lower Bound (ELBO):

$$-D_{KL}(q_\phi(\tau|\mathbf{x}, \mathbf{y}, \mathcal{G})||\mathcal{N}(0, I)) + \frac{1}{P} \sum_{i=1}^P \log p_\Theta(\hat{\mathbf{y}}|\tau^{(i)}, \mathbf{x}, \mathcal{G}) \quad (5)$$

During inference, only the decoder is used to predict the distribution of critical nodes for a given planning problem when samples are drawn from $\mathcal{N}(0, I)$. The GNN-CVAE improves over the GNN and GAT models in that it predicts a probability distribution of critical nodes instead of a single point which is often more desirable in a planning problem. For example, all points inside the narrow corridor in Fig 3 are vital as any of them can cause a collision instead of considering only one single point. We compare these GNN based models against a CNN variant where all the GNN layers are replaced by CNNs and a CVAE which has a mix of CNN/FCN layers depending on the problem.

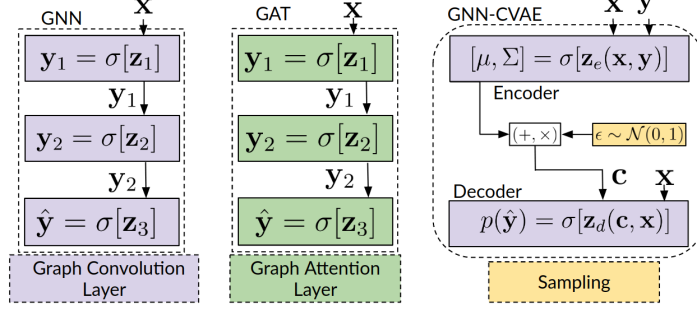


Figure 2: **GNN Architectures for Motion Planning.** a) GNN model consisting of multiple layers of graph convolution. The last layer directly outputs \hat{y} . b) GAT model consists of multiple layers of the attention weighted graph convolution [18] and the final layer directly outputs \hat{y} . c) **GNN-CVAE** uses graph convolutions in the in the encoder and decoder of a conditional variational auto-encoder.

3.2 Identifying Critical Samples

We consider a two dimensional space populated with corridors as seen in Fig 3. such that all points in the space exist between (0,0) to (1,1). The walls are randomly generated resulting in random narrow corridors. The space is covered with a r -disc Halton graph with 2000 vertices in \mathbb{R}^2 . This graph remains constant even when the planning problem changes. The graph is found to be dense enough to cover any planning problem in this space. Node n is equipped with a feature vector $\mathbf{x}_n = [x_n, x_{init}, x_{goal}, f_n]$ where x_n is robot n 's position in the plane and f_n is a feature indicator for node n . In the simplest case, f_n can represent whether node n is occupied.

The dataset generated for training consists of 400 randomly generated maps and start and goal locations. In the case that for a given motion planning problem \mathbf{M} where the ground truth algorithm generates more than one bottleneck node inside the narrow corridor, each bottleneck node can serve as a training label for \mathbf{M} . In total the training set consists of 15000 samples from which a train/validate/test split is performed. Fig 3 is indicative of our qualitative findings. We make the following observations: In most cases the CNN architecture is unable to transfer to the new environments that are significantly different from the ones observed during training. The GNN and GAT architectures are able to handle the multiple wall scenarios and produce critical nodes that are close to the ground truth critical node. The CVAE tends to be more robust than the CNN architecture. However, the distribution of the critical nodes predicted by the CVAE tends to have most of its mass concentrated at a single point. On the other hand GNN-CVAE paints a richer picture of the passageway with most of the probability mass lying close to the bottleneck node (Fig 3). We initially hypothesized that planning on graphs with GNNs could possibly outperform CNN/FCN architectures since the graph representation captures a richer picture of the planning problem and would be more robust to changes in the planning space. For example, a single pixel change can be used to fool CNNs [21]. For planning algorithms that operate in dynamic environments in the real world, they must be at the very least robust to small perturbations in the environment.

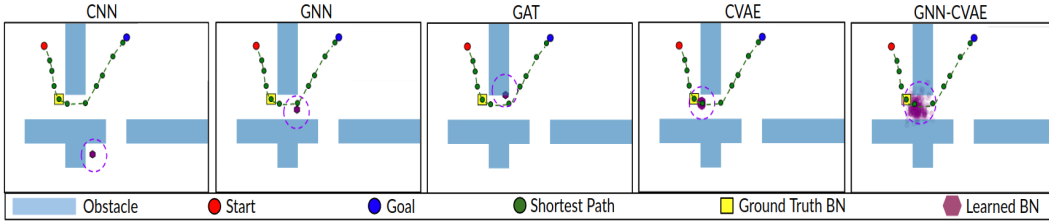


Figure 3: **Learning Critical Samples.** CNN architectures are unable to predict critical nodes but GNN and GAT architectures can predict critical node with a small margin of error. CVAE predicts a probability distribution with most of the mass is concentrated at one point while GNN-CVAE provides a richer picture of the narrow passageway.

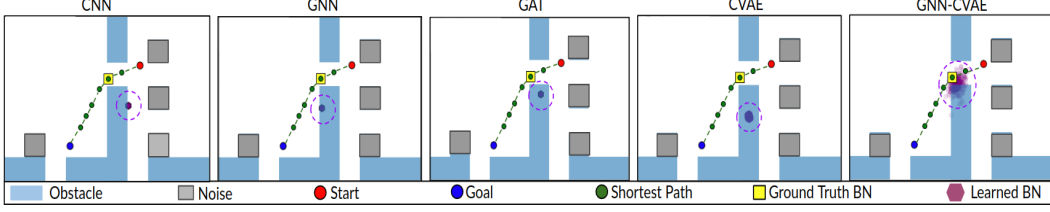


Figure 5: **Critical Samples on Corrupted Data.** On maps corrupted with random blobs not present during training, only the GNN-CVAE can predict an accurate distribution of critical nodes.

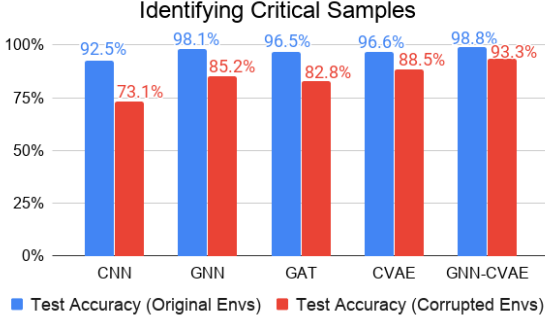


Figure 4: **Identifying Critical Samples.** Test accuracy averaged over 300 distinct planning problems.

To evaluate robustness, we test these graph architectures on environments corrupted by random blobs not present in training (Fig 5). Even the CVAE architecture is unable to handle these perturbations and only the GNN-CVAE is able accurately predict a distribution centered around the ground truth bottleneck node (Fig 5). We report accuracy as the complement of the mean squared error between the predicted \hat{y} and the ground truth y in Fig 4. We conclude from these experiments that GNNs and GNN-CVAEs offer qualitative as well as quantitative advantages over CNN/FCN architectures for identifying critical nodes.

4 Learning Value Functions with Graph Neural Networks

Using GNNs to identify critical samples reduces the complexity of the planning problem. However, it cannot be guaranteed that the critical nodes generated by GNNs/CNNs are always correct and can sometimes predict critical nodes placed inside obstacles which can result in catastrophic failures. Instead, in this section we look to use GNNs as guiding functions for search algorithms that are complete, i.e guaranteed to find a collision free path if one exists. More concretely, we consider the \mathbb{R}^2 space from Section 3.2 equipped with a dense graph \mathcal{G} . For a given planning problem \mathbf{M} on, we look to run A^* on the graph \mathcal{G} . A^* differs from an uninformed search algorithm such as Dijkstra’s in that it requires a heuristic to guide the search. In a \mathbb{R}^2 space it is common practice to use the distance between the current node and the goal node as the heuristic. However, in scenarios such as cul-de-sacs or flytrap environments (environments with long dead end tunnels) the L2 distance can guide the search algorithm in the wrong direction. Designing a good heuristic that fits all scenarios can be an extremely challenging problem [3]. We hypothesize that information inferred from the local graph topology is better suited at guiding a search algorithm. Thus, we look to learn heuristic or value functions with GNNs. These heuristics are then used by the search algorithm to find a path \mathbf{p} . If the graph search algorithm $\mathbf{A}(\mathcal{G}, \mathbf{M})$ defined in Sec 3 is extended to represent A^* and a function of the heuristic h , i.e $\mathbf{A}(\mathcal{G}, \mathbf{M}, h)$ and $c(\mathbf{A})$ is extended to represent cost of running A^* then the problem statement considered in this section can be given as:

Problem 2. For a given planning problem $\mathbf{M} = \{\mathcal{X}_{free}, x_{init}, x_{goal}\}$ on \mathcal{G} , compute a heuristic $h := \Lambda(x, x_g) \forall x \in \mathcal{X}_{free}$, that minimizes the ratio of the costs of running $\mathbf{A}(\mathcal{G}, \mathbf{M}, h)$ to the cost of running $\mathbf{A}(\mathcal{G}, \mathbf{M}, h_2)$ where h_2 is the L2 distance heuristic.

$$\Lambda^* = \operatorname{argmin}_{\Lambda} \left[\frac{c(\mathbf{A}(\mathcal{G}, \mathbf{M}, \Lambda))}{c(\mathbf{A}(\mathcal{G}, \mathbf{M}, h_2))} \right] \quad (6)$$

To study the ability of GNNs to learn topological information that guides graph search better than the L2 heuristic, we again choose the 3 architectures from Sec. 3.1.

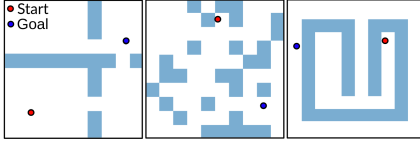


Figure 6: **Test Environments.** L) Test Env C) Corrupted Env R) FlyTrap Env

The same r -disc Halton graph with 2000 vertices in \mathbb{R}^2 from Sec. 3.2 is reused. Node n is equipped with a feature vector $\mathbf{x}_n = [x, x_n, x_{goal}, f_n]$ where x is the current node popped from the frontier, x_n is the current node’s position and f_n is a feature indicator for node n as before. Training data is generated by running Dijkstra’s algorithm for a given x_{init} and x_{goal} and is used to compute the shortest path \mathbf{p}^* . Then for every $x \in \mathbf{p}^*$ the cost to reach the goal given by $c(x_n, x_{goal})$ serves as the training label. The training set is biased to only contain samples from relevant

path nodes in order to reduce the amount of information that the networks must learn over. In order to study the ability of GNN-based policies to transfer to new environments, we train on environments with linear walls with a gap but test on more challenging environments; an environment with multiple gaps, a test environment corrupted with randomly generated blobs and a flytrap environment with long tunnels (Fig 6). Since the time complexity of the A^* depends on the depth of the computed solution and the branching factor [2], the performance of the learned heuristics is judged by looking at two key parameters; the number of nodes expanded and the length of the paths generated. We observe

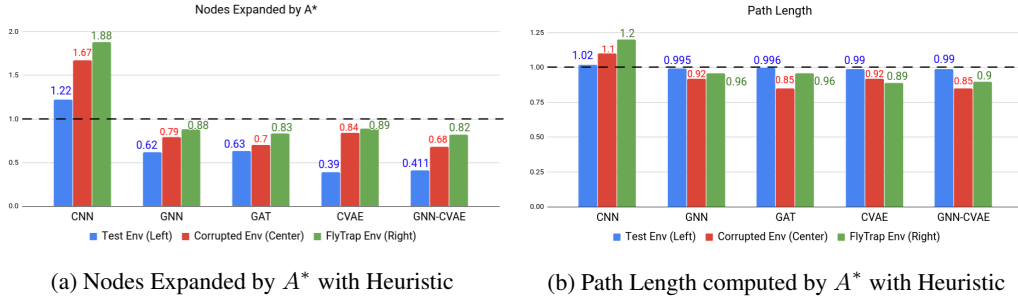


Figure 7: **Metrics for A^* with Learned Heuristics** Each bar shows the ratio of the heuristic’s metric to the L2 heuristic produced by running over 300 runs. Metric greater than 1 implies performance worse than L2. Lower numbers are more desirable for both metrics.

from Fig 7a that A^* with the CNN heuristic always expands more nodes for all three environments while GNN and GAT architectures have comparable performance to the CVAE architecture. The GNN-CVAE outperforms all others on all three environments. From Fig 7b we observe that for the simple environments (test and corrupted) the path length produced by the heuristic is very close to the path length produced by L2 distance. However, in the flytrap environment the L2 distance can be misleading since following the L2 distance can lead to dead-ends. Here, we observe again that the GNN-CVAE offers the highest performance gains over a naive L2 heuristic and other learned heuristics. Thus, from these results we conclude GNNs and GNN-CVAE offer significant advantages for learning robust value functions informed by underlying graph topology.

5 Learning Sampling Distributions with Graph Neural Networks

In Sec 3.2 and 4 we operate under the assumption that the planning space can be discretized and be covered by a dense graph. The discretization assumption can break down for robots with kinodynamic constraints. The graph \mathcal{G} covering the planning space $\mathcal{X} \in \mathbb{R}^d$ can require a very large number of nodes for dense coverage if d increases by even one or two dimensions, thus making the problem of learning over the graph much harder. To overcome these challenges we look to adapt our GNN solutions to Sampling-based Planners (SBPs). Concretely, we consider Rapidly-exploring Random Trees (RRTs) that build an online graph by directly (uniformly) sampling the C-space.

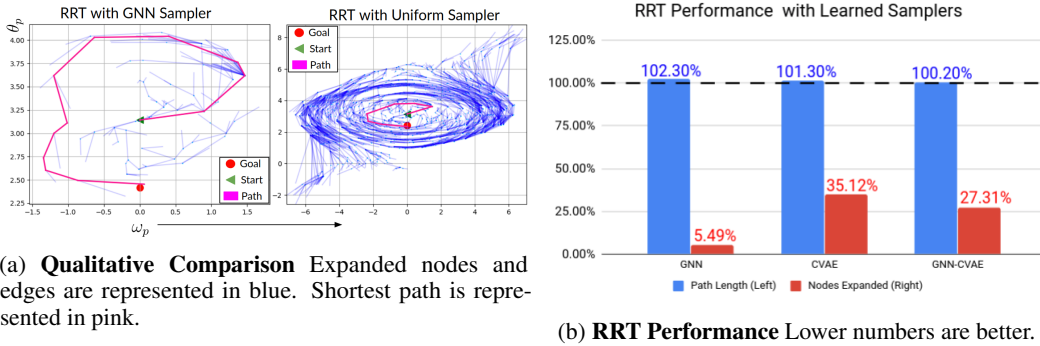
In order to study a problem with kinodynamic constraints that is non-trivial to discretize we move away from the 2D planar navigation and instead consider a pendulum system. The pendulum starts at the bottom and is given a desired angle and velocity as the goal to be achieved. The pendulum is control limited and must plan a path that increases energy till the desired goal can be reached. The state of the system is given by $x = [\theta_p, \omega]$ where θ_p is the angle the pendulum makes with the horizontal and the angular velocity ω of the pendulum taken about its center of mass. Formally, if

the samples $[x_1, x_2, \dots] \sim \mu$ in the SBP are drawn from a distribution μ and the search algorithm $\mathbf{A}(\mathbf{M}, x_1, x_2, \dots)$ is extended to be a function of \mathbf{M} as well as the samples (x_1, x_2, \dots) , then the problem considered in this section is:

Problem 3. For planning problem \mathbf{M} and a given SBP search algorithm \mathbf{A} compute parameters of the distribution μ from which states $[x_1, x_2, \dots]$ are sampled during execution of \mathbf{A} such that the cost c of running $\mathbf{A}(\mathbf{M}, x_1, x_2, \dots)$ is minimized;

$$\mu^* = \underset{\mu}{\operatorname{argmin}} \mathbb{E}_{\{\mathbf{M}, \mu\}} \left[c(\mathbf{A}(\mathbf{M}, x_1, x_2, \dots)) \right] \quad (7)$$

For a given \mathbf{M} , the graph \mathcal{G} is initialized with the start node x_{init} and a collection of m -nearest nodes connected to the start node. Nodes are added to the graph from the sampler μ . It is important to note that in this section, the graph \mathcal{G} is *not constant* for over all \mathbf{M} and is instead constructed as the RRT tree expands. This significantly increases the difficulty of the learning problem because now the GNNs must learn to infer the topology of the problem through a time varying graph. The features of node n are given as $\mathbf{x}_n = [x_n, x_{init}, x_{goal}]$ where x_n represents the state of the pendulum system at node n . For this problem, we only consider the GNN, CVAE and GNN-CVAE architectures. We report results in Fig 8. The generative architectures CVAE/GNN-CVAE offer a smaller benefit for the online planning case when compared to the GNN architecture. However, all three architectures improve upon the uniform sampler by expanding far fewer nodes and edges to produce essentially equivalent paths to the goal. We conclude that learning sampling distributions with GNNs can offer substantial benefits over uniform samplers and FCN architectures in SBPs.



(a) **Qualitative Comparison** Expanded nodes and edges are represented in blue. Shortest path is represented in pink.

(b) **RRT Performance** Lower numbers are better.

Figure 8: **Qualitative and Quantitative Comparison of RRT with Learned Samplers** a) When compared to the Uniform Sampler, the GNN sampler expands significantly lesser number of nodes. b) Each bar shows the percentage of the samplers metric to the uniform sampler heuristic produced by running over 300 runs. Metric greater than 100% implies performance worse than uniform sampler.

6 Conclusion

GNNs offer a natural way to express functions in graph based planning and can be adapted to a variety of motion planning problems with ease. Three GNN-based architectures are proposed namely, GNN, GAT and GNN-CVAE for motion planning problems, including a densely sampled static graph for low-dimensional problems and a dynamically sampled graph for high-dimensional problems with kinodynamic constraints. We find that the GNN-CVAE model substantially outperforms CNN methods for learning critical samples and value functions while GNNs outperform more powerful generative models that use fully-connected networks for high-dimensional sampling-based planning.

While there still exists the difficulty of adapting learning methods to very high-dimensional planning problems, nevertheless we foresee many avenues for these methods to be extended. State vectors for robots can be replaced directly with sensor readings such as lidars or even downstream image features from a cameras. The online sampling distribution can be improved upon and adapted to handle long navigation by methods such as pruning the tree. We leave these for future work.

7 Broader Impact Statement

In this work, we propose looking at motion planning problems in a different light. Since most motion planning problems involve searching on graphs, we focus on using Graph Neural Networks instead of Convolutional Neural Networks or Fully Connected Networks. Such an approach can be easily extended to self-driving approaches. In light of some of the recent failures of CNN based approaches in self-driving due to perturbations in the image sensors, we hope planning methods that use a GNN in the loop can provide an additional layer of safety. Improved safety in self-driving technology could possibly lead to wider adoption of autonomous vehicles resulting in a loss of jobs such as delivery drivers, rideshare drivers etc. reliant on these jobs for their livelihoods and thus, such advances must be carefully balanced.

References

- [1] Jean-Claude Latombe. Motion planning: A journey of robots, molecules, digital actors, and other artifacts. *The International Journal of Robotics Research*, 18(11):1119–1128, 1999.
- [2] Stuart Russell and Peter Norvig. Artificial intelligence: a modern approach. 2002.
- [3] Blai Bonet and Héctor Geffner. Planning as heuristic search. *Artificial Intelligence*. 2001 Jun; 129 (1-2): 5-33., 2001.
- [4] Steven M LaValle. *Planning algorithms*. Cambridge university press, 2006.
- [5] David Hsu, J-C Latombe, and Rajeew Motwani. Path planning in expansive configuration spaces. In *Proceedings of International Conference on Robotics and Automation*, volume 3, pages 2719–2726. IEEE, 1997.
- [6] Brian Ichter, James Harrison, and Marco Pavone. Learning sampling distributions for robot motion planning. In *2018 IEEE International Conference on Robotics and Automation (ICRA)*, pages 7087–7094. IEEE, 2018.
- [7] Hao-Tien Lewis Chiang, Jasmine Hsu, Marek Fiser, Lydia Tapia, and Aleksandra Faust. RL-rrt: Kinodynamic motion planning via learning reachability estimators from rl policies. *IEEE Robotics and Automation Letters*, 4(4):4298–4305, 2019.
- [8] Clark Zhang, Jinwook Huh, and Daniel D Lee. Learning implicit sampling distributions for motion planning. In *2018 IEEE/RSJ International Conference on Intelligent Robots and Systems (IROS)*, pages 3654–3661. IEEE, 2018.
- [9] Brian Ichter, Edward Schmerling, Tsang-Wei Edward Lee, and Aleksandra Faust. Learned critical probabilistic roadmaps for robotic motion planning. *arXiv preprint arXiv:1910.03701*, 2019.
- [10] Rahul Kumar, Aditya Mandalika, Sanjiban Choudhury, and Siddhartha S Srinivasa. Lego: Leveraging experience in roadmap generation for sampling-based planning. *arXiv preprint arXiv:1907.09574*, 2019.
- [11] Thomas N Kipf and Max Welling. Semi-supervised classification with graph convolutional networks. *arXiv preprint arXiv:1609.02907*, 2016.
- [12] Alex Fout, Jonathon Byrd, Basir Shariat, and Asa Ben-Hur. Protein interface prediction using graph convolutional networks. In *Advances in neural information processing systems*, pages 6530–6539, 2017.
- [13] Zhouxia Wang, Tianshui Chen, Jimmy Ren, Weihao Yu, Hui Cheng, and Liang Lin. Deep reasoning with knowledge graph for social relationship understanding. *arXiv preprint arXiv:1807.00504*, 2018.
- [14] Arbaaz Khan, Ekaterina Tolstaya, Alejandro Ribeiro, and Vijay Kumar. Graph policy gradients for large scale robot control. *arXiv preprint arXiv:1907.03822*, 2019.

- [15] Fernando Gama, Joan Bruna, and Alejandro Ribeiro. Stability properties of graph neural networks. *arXiv preprint arXiv:1905.04497*, 2019.
- [16] Fernando Gama, Antonio G Marques, Geert Leus, and Alejandro Ribeiro. Convolutional neural network architectures for signals supported on graphs. *IEEE Transactions on Signal Processing*, 67(4):1034–1049, 2018.
- [17] Santiago Segarra, Antonio G Marques, and Alejandro Ribeiro. Optimal graph-filter design and applications to distributed linear network operators. *IEEE Transactions on Signal Processing*, 65(15):4117–4131.
- [18] Petar Veličković, Guillem Cucurull, Arantxa Casanova, Adriana Romero, Pietro Lio, and Yoshua Bengio. Graph attention networks. *arXiv preprint arXiv:1710.10903*, 2017.
- [19] Lucas Janson, Brian Ichter, and Marco Pavone. Deterministic sampling-based motion planning: Optimality, complexity, and performance. *The International Journal of Robotics Research*, 37(1):46–61, 2018.
- [20] Kihyuk Sohn, Honglak Lee, and Xinchen Yan. Learning structured output representation using deep conditional generative models. In *Advances in neural information processing systems*, pages 3483–3491, 2015.
- [21] Jiawei Su, Danilo Vasconcellos Vargas, and Kouichi Sakurai. One pixel attack for fooling deep neural networks. *IEEE Transactions on Evolutionary Computation*, 23(5):828–841, 2019.

8 Appendix

8.1 Additional Results and Details

In the experiments presented in Section 3 and Section 4 the space \mathbb{R}^2 is covered by a graph \mathcal{G} . As mentioned in the body of the main paper, this \mathcal{G} is taken to be sufficiently dense such that any planning problem in \mathbb{R}^2 can be represented on \mathcal{G} . A visualization of this can be seen in Fig. 9

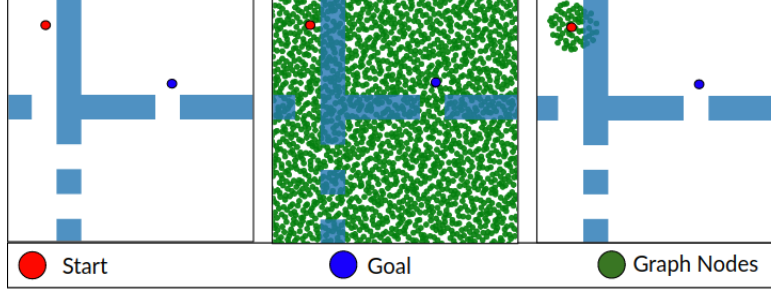


Figure 9: **Graph Visualization for problems in \mathbb{R}^2 .** The planning problem on the left is overlaid with a graph \mathcal{G} . We omit the edges for ease of visualization. The nodes connected to the start node are shown on the right.

For a planning problem M , node n 's feature f_n can be simply computed by checking if node n is occupied or not. A caveat of such an approach is that the number of nodes in the graph required to cover a d -dimensional space increases as d increases, thus motivating a shift towards sample based planning.

8.2 Qualitative Results for Learning Heuristics with Graph Neural Networks

In Section 4, we presented quantitative results for learning heuristics with graph neural networks. We showed that on average GNN's are able to expand significantly lower number of nodes as compared to a naive L2 heuristic. The planning space in Fig. 10 left, represents one of the more challenging

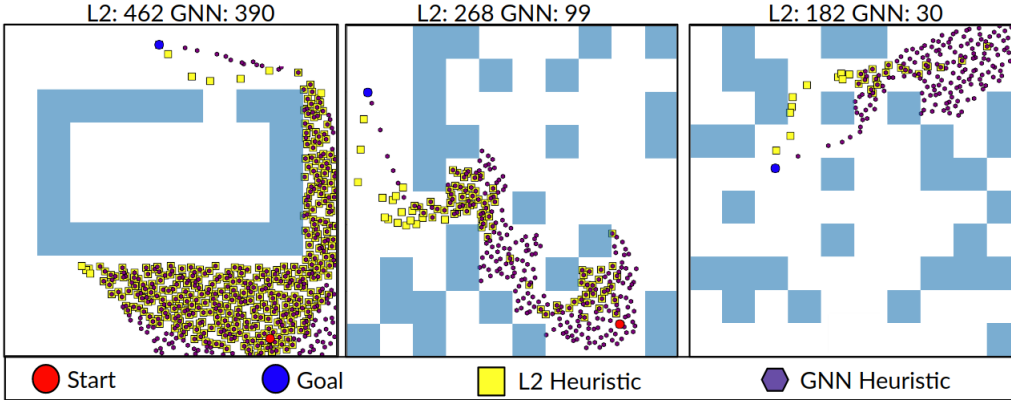


Figure 10: **Qualitative results for learning heuristics** The nodes expanded by A^* when using the L2 heuristic as compared to when using the GNN heuristic is given at the top.

problems since most of the space is blocked off and only a narrow opening presents a viable path to the goal. In such a setting the GNN heuristic offers only modest gains over the L2 heuristic. For the planning spaces in Fig 9 center and right, the GNN is able to better select those nodes that lead directly to the goal by utilizing the overall graph structure. This leads it to expand significantly smaller number of nodes.

9 Training and Inference Methodologies

The training methodology for predicting critical nodes is fairly straightforward. For a given planning problem \mathbf{M} , the shortest path \mathbf{p} is computed using any graph search algorithm. The bottleneck node algorithm of [10] takes in as input \mathbf{M} , \mathcal{G} and the path \mathbf{p} to produce ground truth critical node \mathbf{y} . In order to produce a dataset for training various graph based frameworks, in an additional step node feature vector \mathbf{x} is generated for \mathbf{M} . The dataset then consists of the tuples $D = \{\{\mathbf{M}_1, \mathbf{x}_1, \mathcal{G}, \mathbf{y}_1\}, \dots, \{\mathbf{M}_N, \mathbf{x}_N, \mathcal{G}, \mathbf{y}_N\}\}$. The critical node predictor is trained on this dataset by minimizing the L2 loss between the predicted samples $\hat{\mathbf{y}}$ and the ground truth samples \mathbf{y} . In the case of the CVAE architectures, the training is done by minimizing the ELBO loss given in Eqn 5. Since the planning space is \mathbb{R}^2 , the dimensionality of the latent space is also set to 2.

During inference, a new planning problem is generated, the graph used during training \mathcal{G} is invoked to compute feature vector \mathbf{x} . \mathcal{G} and \mathbf{x} are fed into the GNN architectures and the output of the GNN is recorded as the predicted critical node. In the case of the CVAE architectures, the latent variable an additional τ is sampled from a normal distribution $\mathcal{N}(0, I)$. The graph \mathcal{G} , \mathbf{x} and τ are fed into the decoder to produce a probability distribution over the estimate of the critical node.

The outline to learn sampling distributions and heuristics is a little more involved. We first present outline the methodology for learning critical nodes in Algorithm 1.

Algorithm 1 Learning Critical Samples.

- 1: **Offline:**
 - 2: Initialize empty dataset $D = \{\}$
 - 3: **for** time $t = [0, \dots, T]$ **do**
 - 4: Initialize planning problem $\mathbf{M} = \{\mathcal{X}_{\text{free}}, x_{\text{init}}, x_{\text{goal}}\}$
 - 5: Use uniform sampler in RRT to compute path \mathbf{p}
 - 6: Initialize graph $\mathcal{G} = x_{\text{init}}$
 - 7: **for** p in range $(0, \text{length}(\mathbf{p})-1)$ **do**
 - 8: Update graph $\mathcal{G} := x_{\text{init}} \oplus \mathbf{p}[p]$
 - 9: Compute feature vector \mathbf{x} for all nodes currently in \mathcal{G} .
 - 10: Generate label $\mathbf{y} = \mathbf{p}[p + 1]$
 - 11: Add to dataset $D := \{\mathcal{G}, \mathbf{x}, \mathbf{y}\}$
 - 12: Train parameters of sampling distribution $\mu(\mathcal{G}, \mathbf{x})$ where inputs are \mathcal{G} and \mathbf{x}
 - 13: **Online:**
 - 14: Initialize new planning problem \mathbf{M} .
 - 15: Randomly sample points s near x_{init}
 - 16: Construct initial graph $\mathcal{G} := x_{\text{init}} \oplus s$
 - 17: Generate \mathbf{x} for all nodes in current graph
 - 18: Predict next node $\hat{\mathbf{y}}$ to expand from $\mu(\mathcal{G}, \mathbf{x})$
 - 19: **while** $\hat{\mathbf{y}} \neq x_{\text{goal}}$ **do**
 - 20: Find node in \mathcal{G} closest to $\hat{\mathbf{y}}$ and generate edge e by integrating through dynamics of system
 - 21: Update graph $\mathcal{G} := \mathcal{G} \oplus \hat{\mathbf{y}}$
 - 22: Recompute \mathbf{x} for updated graph
 - 23: Predict new $\hat{\mathbf{y}}$ from $\mu(\mathcal{G}, \mathbf{x})$
-

A similar approach can be followed for learning heuristics. In the dataset creation step, instead of recording the next node as the target, the cost of reaching the goal from nodes in the path is recorded as the label. Further, the graph is fixed for the whole system.

During inference, when A^* looks to expand to pick the new best node to expand, the GNN is used to predict the heuristic. In practice to produce best results we use a weighted combination of the L2 distance and the heuristic similar to the approach in [6].